Neural and endocranial anatomy of Triassic phytosaurian reptiles and convergence with fossil and modern crocodylians

Stephan Lautenschlager [Corresp., 1] , Richard Butler [2]

[1] School of Earth Sciences, University of Bristol, Bristol, United Kingdom

[2] School of Geography, Earth and Environmental Sciences, University of Birmingham, Birmingham, United Kingdom

Corresponding Author: Stephan Lautenschlager
Email address: glzsl@bristol.ac.uk

Phytosaurs are a clade of large, carnivorous pseudosuchian archosaurs from the Late Triassic with a near cosmopolitan distribution. Their superficial resemblance to longirostrine (long-snouted) crocodylians, such as gharials, has often been used in the past to infer ecological and behavioural convergence between the two groups. Although more than thirty species of phytosaur are currently recognised, little is known about the endocranial anatomy of this clade. Here, we describe the endocranial anatomy (including the brain, inner ear, neurovascular structures and sinus systems) of the two non-mystriosuchine phytosaurs *Parasuchus angustifrons* (="*Paleorhinus angustifrons*") and *Ebrachosuchus neukami* from the Late Triassic of Germany based on digital reconstructions. Results show that the endocasts of both taxa are very similar to each other in their rostrocaudally elongate morphology, with long olfactory tracts, weakly demarcated cerebral regions and dorsoventrally short endosseous labyrinths. In addition, several sinuses, including large antorbital sinuses and prominent dural venous sinuses, were reconstructed. Comparisons with the endocranial anatomy of derived phytosaurs indicate that Phytosauria is united by the presence of elongate olfactory tracts and longitudinally arranged brain architecture - characters which are also shared with Crocodyliformes. However, a substantial morphological variability is observed in the cephalic and pontine flexure and the presence of a pineal organ across the different phytosaur species. These results suggest that the endocranial anatomy in Phytosauria generally follows a plesiomorphic pattern, with moderate variation within the clade likely resulting from divergent sensory and behavioural adaptations.

1   **Neural and endocranial anatomy of Triassic phytosaurian reptiles and convergence with**
2   **fossil and modern crocodylians**

3

4   **Stephan Lautenschlager[1]*, Richard J. Butler[2]**

5

6   *[1]School of Earth Sciences, University of Bristol, Life Sciences Building, Bristol BS8 1TQ, UK*

7   *[2]School of Geography, Earth and Environmental Sciences, University of Birmingham,*

8   *Birmingham B15 2TT, UK*

9

10   *Corresponding author: Stephan Lautenschlager, glzsl@bristol.ac.uk, +44 (0) 117 331 5239*

11

12   Short title: Neuroanatomy of Phytosauria

13

14 **ABSTRACT**

15

16 Phytosaurs are a clade of large, carnivorous pseudosuchian archosaurs from the Late Triassic

17 with a near cosmopolitan distribution. Their superficial resemblance to longirostrine (long-

18 snouted) crocodylians, such as gharials, has often been used in the past to infer ecological and

19 behavioural convergence between the two groups. Although more than thirty species of

20 phytosaur are currently recognised, little is known about the endocranial anatomy of this clade.

21 Here, we describe the endocranial anatomy (including the brain, inner ear, neurovascular

22 structures and sinus systems) of the two non-mystriosuchine phytosaurs *Parasuchus angustifrons*

23 (=“*Paleorhinus angustifrons*”) and *Ebrachosuchus neukami* from the Late Triassic of Germany

24 based on digital reconstructions. Results show that the endocasts of both taxa are very similar to

25 each other in their rostrocaudally elongate morphology, with long olfactory tracts, weakly

26 demarcated cerebral regions and dorsoventrally short endosseous labyrinths. In addition, several

27 sinuses, including large antorbital sinuses and prominent dural venous sinuses, were

28 reconstructed. Comparisons with the endocranial anatomy of derived phytosaurs indicate that

29 Phytosauria is united by the presence of elongate olfactory tracts and longitudinally arranged

30 brain architecture - characters which are also shared with Crocodyliformes. However, a

31 substantial morphological variability is observed in the cephalic and pontine flexure and the

32 presence of a pineal organ across the different phytosaur species. These results suggest that the

33 endocranial anatomy in Phytosauria generally follows a plesiomorphic pattern, with moderate

34 variation within the clade likely resulting from divergent sensory and behavioural adaptations.

35

36 **INTRODUCTION**

37 Phytosaurs are a group of fossil archosauriform reptiles commonly found in Upper Triassic (c.

38 235–202 Ma) sediments in North America and Europe, and less commonly in other regions such

39 as India, Africa, East Asia, Madagascar and South America (Stocker and Butler, 2013).

40 Phytosaurs have usually been regarded as the earliest diverging group within the crocodylian

41 stem-lineage Pseudosuchia (Sereno, 1991; Parrish, 1993; Brusatte et al., 2010; Ezcurra 2016),

42 which together with Avemetatarsalia (pterosaurs, dinosaurs, birds) form the clade Archosauria.

43 One recent phylogenetic dataset has recovered Phytosauria as a monophyletic clade just outside

44 of and as a sister taxon to Archosauria (Nesbitt, 2011), although this result has not been

45 supported by a recent comprehensive revision of the phylogeny of early archosauriforms

46 (Ezcurra, 2016). Morphologically, phytosaurs resemble extant crocodylians, particularly

47 longirostrine morphotypes such as gharials. Members of both groups possess large elongate

48 skulls equipped with conical teeth, rows of sculptured osteoderms covering the axial and

49 appendicular skeleton, and are characterised by a quadrupedal, sprawling gate (Westphal, 1976).

50 Evidence from taphonomy and ichnofossils suggests that, similar to crocodylians, phytosaurs

51 were generally aquatic or semi-aquatic (Buffetaut, 1993; Renesto and Lombardo, 1999), but

52 were also capable of terrestrial locomotion (Parrish, 1986). Although phytosaurs and the earliest

53 fossil crocodylians are significantly separated temporally (by about 100 million years) and

54 phylogenetically, gross morphological similarities between the two groups have often been cited

55 as evidence for ecological and behavioural convergence (Camp, 1930; Anderson, 1936; Hunt,

56 1989; Hungerbühler, 2002; Witzmann et al., 2014). However, phytosaurs are defined by a

57 number of osteological characters that differentiate them from crocodylians, such as an elongate

58 premaxilla, the caudal position of the external nares (which is placed close to the orbit in

59   phytosaurs, rather than at the tip of the rostrum), and the absence of a secondary palate.

60   Convergence in the form of a longirostrine skull shape has occurred numerous times throughout

61   the evolution of pseudosuchian archosaurs (Brochu, 2001); presumably as an adaptation to a

62   specific habitat and diet (e.g. piscivory) (Pierce et al., 2008). However, the extent to which this

63   osteological convergence is also reflected in soft-tissue structures, such as the endocranial

64   anatomy, remains unclear. Neuroanatomical adaptations to a specific ecology or behaviour in

65   phylogenetically divergent groups as drivers for morphological similarities have been suggested

66   in avemetatarsalian ("bird-line") archosaurs (Witmer et al., 2003).

67   In the past, research on phytosaurs has largely focussed on comparative osteology,

68   taxonomy and phylogenetic relationships. Due to their near-global geographic distribution but

69   restricted temporal distribution phytosaurs have been used as index fossils in biostratigraphy. In

70   comparison, the reconstruction and study of the endocranial anatomy of phytosaurs has received

71   little attention (e. g. Cope, 1888; Case, 1928; Mehl, 1928; Camp, 1930; Chatterjee, 1978). Most

72   recently, Holloway et al. (2013) described a digital endocast of the derived mystriosuchine

73   phytosaur *Machaeroprosopus mccauleyi* (=*"Pseudopalatus mccauleyi"*) in order to evaluate the

74   evolution of sensory systems in archosaurs.

75   Here, we describe the endocranial anatomy (including the brain, inner ear, neurovascular

76   structures and sinus systems) of the two non-mystriosuchine phytosaurs *Parasuchus angustifrons*

77   (=*"Paleorhinus angustifrons"*) and *Ebrachosuchus neukami* (Butler et al., 2014; see Kammerer

78   et al. 2016 for recent taxonomic revisions) (Fig. 1) based on digital reconstructions. Further

79   comparisons are made with existing reconstructions for other phytosaurian and crocodylian taxa.

80

81   **MATERIALS AND METHODS**

82 **Specimens**

83 The studied specimens consist of the holotypes of *Ebrachosuchus neukami* (BSPG 1931 X 501;

84 Bayerische Staatssammlung für Paläontologie und Geologie, Munich, Germany) and *Parasuchus*

85 *angustifrons* (BSPG 1931 X 502) (Kuhn 1936; Butler et al., 2014). The skull of *Ebrachosuchus*

86 *neukami* is fully articulated and complete and preparation work has removed most of the

87 sandstone matrix, with the exception of most internal cavities, which remain filled with matrix.

88 The skull of *Parasuchus angustifrons* is articulated and mostly complete apart from the

89 premaxilla, of which only a small portion immediately rostral to the external nares is preserved.

90 Sandstone matrix remains within most of the internal cavities. Both of the skulls have undergone

91 some plastic deformation, primarily in the form of dorsoventral compression, but are otherwise

92 remarkably well preserved, with minimum transverse distortion. Brittle deformation and

93 fracturing are largely absent.

94

95 **CT scanning and digital reconstruction**

96 The holotypes of *Ebrachosuchus neukami* (BSPG 1931 X 501) and *Parasuchus angustifrons*

97 (BSPG 1931 X 502) were scanned at the Klinikum rechts der Isar (Munich) using a Siemens

98 SOMATOM Sensation 64 CT scanner. Datasets consisted of 1634 slices (512 x 512 x 1634

99 pixels, 0.6 mm voxel size) for *Ebrachosuchus neukami* and 809 slices (512 x 512 x 1634 pixels,

100 0.6 mm voxel size) for *Parasuchus angustifrons*. CT data sets are deposited with the specimens

101 in the BSPG collections and on Fgshare.(https://figshare.com/).

102 The respective CT data files were imported into Avizo 7.0 (Visualisation Science Group)

103 for image segmentation and digital reconstruction. Anatomical structures of interest (endocasts,

104 endosseous labyrinths, neurovascular and sinus structures) were labelled using Avizo's

105   segmentation editor. The magic wand tool was used where possible to perform the segmentation

106   semi-automatically. In regions with poor contrast between matrix, bone and structures of interest

107   the paintbrush tool was used for manual segmentation. 3D surface models and volumes were

108   created to visualize the segmented structures and to illustrate this article with traditional figures.

109   In addition, surface models of the individual structures were downsampled to a degree that

110   allowed for small file sizes but preserved all details, and were exported as separate OBJ files for

111   the creation of the interactive 3D figures in the supplementary material as outlined in

112   Lautenschlager (2014) using Adobe 3D reviewer (Adobe Systems Inc.).

113   As both taxa have been compressed dorsoventrally to a moderate amount, the resulting

114   endocasts were retrodeformed. For the retrodeformation process, the digital skull and endocast

115   models were scaled in dorsoventral direction using the "transform editor" in Avizo. BSPG 1931

116   X 502 was scaled to the same dorsoventral dimensions as a less compressed skull of *Parasuchus*

117   *hislopi* (ISI R42, Indian Statistical Institute, Kolkata, India), corresponding to a scaling factor of

118   approximately 40%. The same scaling factor was assumed for BSPG 1931 X 501 based on the

119   fact that both specimens were found in close proximity to one another on a single bedding plane

120   and likely had a similar diagenetic history (Butler et al., 2014).

121

122   **Anatomical abbreviations**

123   **airw**, airway; **antorb**, antorbital sinus; **c**, cochlear duct; **car**, carotid artery; **cer**, cerebral

124   hemisphere; **crc**, crus communis; **csc**, caudal semicircular canal; **cvcm**, caudal middle cerebral

125   vein; **dsl**, diverticulum of longitudinal sinus; **dur**, dural venous sinus; **ecto**, ectotympanic sinus;

126   **fl**, floccular lobe; **fv**, fenestra vestibuli; **lab**, endosseous labyrinth; **lsc**, lateral semicircular canal;

127   **nvc**, neurovascular canal; **ob**, olfactory bulbs; **ot**, olfactory tracts; **pit**, pituitary fossa; **pmx**,

128   premaxillary sinus; **rsc**, rostral semicircular canal; **IV**, trochlear nerve canal; V_1, ophthalmic

129   branch of the trigeminal nerve canal; V_2, maxillary branch of the trigeminal nerve canal; V_3,

130   mandibular branch of the trigeminal nerve canal; **VI**, abducens nerve canal; **VII**, facial nerve

131   canal; **IX–XI**, shared canal for the glossopharyngeal, vagus and spinal accessory nerve; **XII**,

132   hypoglossal nerve canal.

133

134   **RESULTS**

135

136   **Endocranial anatomy**

137   The endocasts of *Ebrachosuchus neukami* and *Parasuchus angustifrons* are very similar in their

138   morphology. Both endocasts are elongate, straight (i.e. arranged horizontally) and mediolaterally

139   narrow (Figs. 2, 3). Long olfactory tracts extend rostrally and are as long as the main portion of

140   the endocasts in each taxon. Fossae for olfactory bulbs are preserved in both taxa, but only in

141   *Parasuchus angustifrons* is a rostral separation into two olfactory bulbs visible (Fig. 2B). The

142   ventral extent could not be reconstructed as no bony structures cover this region. The cerebrum

143   and the cerebral hemispheres are only weakly demarcated and form the widest part of the

144   endocast in each taxon. Again, in *Parasuchus angustifrons* the cerebral hemispheres are slightly

145   more prominent than in *Ebrachosuchus neukami*. The mid- and hindbrain region, including the

146   cerebellum, is mediolaterally compressed between the endosseous labyrinths in both taxa.

147   Caudally, the endocasts increase in width towards the foramen magnum. The floccular lobes,

148   extending from the cerebellum, are prominent but short. In comparison to the more oval-shaped

149   morphology in *Parasuchus angustifrons*, the floccular lobes are slightly dorsoventrally flattened

150   in *Ebrachosuchus neukami* (Fig. 3A). In both taxa, the floccular lobes enter the vestibular

151   apparatus of the endosseous labyrinth, but do not extend beyond the rostral semicircular canal.

152   Despite the elongate morphology of the endocasts, the cephalic flexure (between the fore- and

153   mid-brain) and the pontine flexure (between the mid- and hindbrain) are pronounced in the

154   endocasts. The cast of the pituitary fossa is prominent and extends ventrally from the ventral

155   surface of the cerebrum. The pituitary fossae have equal dimensions and positions in both taxa.

156   The canals of the neurovascular structures were reconstructed for as far as indicated by

157   osteological correlates. Their arrangement and dimensions are similar in *Ebrachosuchus neukami*

158   and *Parasuchus angustifrons*. The optic nerve (CN II) and the oculomotor nerve (CN III) canals

159   could not be traced due to the lack of preserved bony structures on the rostroventral part of the

160   endocasts. The trochlear nerve canal (CN IV) is small and originates from the ventral surface of

161   the cerebrum, rostral to the trigeminal nerve (CN V). The latter is prominent in both taxa and

162   originates from the ventrolateral surface of the midbrain region. A split into a rostrally directed

163   ophthalmic branch (CN V_1) and a laterally projecting combined canal for the maxillary (CN V_2)

164   and mandibular (CN V_3) branches is evident in both endocasts. A subdivision of the latter two is

165   not visible in the CT scans, but most likely occurred further outside of the endocranial cavity as

166   is the plesiomorphic archosaurian condition (Witmer et al., 2008). The canal for the abducens

167   nerve (CN VI) originated from the ventral surface of the endocast below the trigeminal nerve

168   canal. The canal for the facial nerve (CN VII) is situated caudal to that of the abducens nerve.

169   The vestibulocochlear nerve canal (CN VIII) could not be reconstructed in either taxon as the

170   resolution of the CT scans is not clear enough in this region to identify the nerve canal

171   confidently. A large metotic fissure is present in both taxa, transmitting the glossopharyngal (CN

172   IX), the vagus (CN X) and the spinal accessory nerves (CN XI). The hypoglossal nerve (CN XII)

173   exits the braincase via a single nerve canal. A further foramen located dorsal to the hypoglossal

174 nerve foramen has a blind ending and likely represents a diverticulum of the longitudinal sinus

175 (Witmer and Ridgely, 2008, 2009).

176   Due to the resolution of the CT data set only the larger vascular structures could be

177 reconstructed. The roots of the caudal middle cerebral vein are prominent and originate from the

178 cerebellum rostrodorsally to the floccular lobes in *Ebrachosuchus neukami* and *Parasuchus*

179 *angustifrons*. They can be traced caudally through the bone for a short extent exiting the

180 braincase near the supraoccipital-parietal suture. Ventrally, the canals for the carotid artery

181 originate from the pituitary fossa and exit the basisphenoid ventrolaterally.

182   In comparison to the other endocranial components, the endosseous labyrinths of

183 *Ebrachosuchus neukami* and *Parasuchus angustifrons* show more prominent differences (Fig. 6).

184 In general, the labyrinths are dorsoventrally short and compact. The vestibular apparatus

185 approaches a rectangular outline and is rostrocaudally elongate in both taxa, but more

186 pronounced in *Ebrachosuchus neukami*. This may partly due to the preservation of *Parasuchus*

187 *angustifrons*, which seems to have been dorsoventrally compacted to a moderate extent (Fig. 6A,

188 B). In *Ebrachosuchus neukami,* the rostral semicircular canal is the longest and describes a

189 somewhat quadrangular shape, whereas the caudal semicircular canal is more oval-shaped (Fig.

190 6C, D). The lateral semicircular canal is short and compact. The semicircular canals in

191 *Parasuchus angustifrons* appear, as far as preserved, dorsoventrally compressed and with more

192 uniform dimension than in *Ebrachosuchus neukami,* although this is partly a preservational

193 artefact. The cochlear ducts are short in *Ebrachosuchus neukami* and *Parasuchus angustifrons*

194 and extend largely ventrally, with only a slight medial component. The fenestra vestibuli were

195 reconstructed in *Ebrachosuchus neukami* and *Parasuchus angustifrons*.

196   As with the endocranial cavities, the arrangement and extent of the various sinuses is

197   similar in *Ebrachosuchus neukami* and *Parasuchus angustifrons* (Fig. 4, 5). The antorbital sinus

198   is large and fills the antorbital fenestra, as well as the space between the palate and the palatal

199   shelf of the maxilla. A small diverticulum also appears to enter the jugal via a foramen near the

200   ectopterygoid-jugal contact (Butler et al., 2014) in both taxa. Rostrally, a large canal is present,

201   which opens into the antorbital cavity. The canal likely transmitted neurovascular structures,

202   including the maxillary branch of the trigeminal nerve. The region rostral to the external nares

203   comprises a large air-filled space for the entire length of the premaxilla medial to the

204   neurovascular canal supplying the alveolar cavities. This region may have housed a premaxillary

205   sinus (most likely as extension of the antorbital sinus) and/or neurovascular bundles (Butler et

206   al., 2014) as in extant crocodiles (Leitch and Catania, 2012). The airway is simple and

207   unbranched in *Ebrachosuchus neukami* and *Parasuchus angustifrons* and connects the external

208   nares with the choanae and the olfactory region.

209   In *Parasuchus angustifrons*, the ectopterygoid is pierced medially by a single oval

210   foramen opening into a large cavity within the bone (Fig. 4). No further foramina are

211   identifiable, suggesting the foramen connected to a pneumatic recess rather than transmitting

212   neurovascular structures. The pneumatic recess is either part of the antorbital sinus or a separate

213   ectopterygoid sinus of unknown source (Witmer, 1997). The respective region is only partly

214   preserved and damaged, but a similarly large cavity appears to be absent in *Ebrachosuchus*

215   *neukami*. A further sinus located dorsal to the brain endocast is present in *Ebrachosuchus*

216   *neukami* and *Parasuchus angustifrons*. While this structure could be interpreted as part of the

217   paratympanic sinus, there is no clear connection to the middle ear visible in the datasets. In both

218   taxa, it covers the cerebellum dorsally. In *Ebrachosuchus neukami* two small diverticula extend

219   rostrally covering the cerebrum dorsolaterally. These diverticula are not visible in *Parasuchus*

220 *angustifrons*. Laterally, subsidiary canals of the tympanic sinus are present in both taxa, but more

221 pronounced in *Parasuchus angustifrons*, in which they exit the braincase via a foramen between

222 the parietal and the prootic and connect to the caudal tympanic recess. This sinus possibly had a

223 further connection to the quadrate foramen, but the pathway for this canal is not indicated by

224 osteological correlates. The sinus is therefore most likely a combination of the endocranium and

225 the dural venous sinuses.

226

227 **Comparison with other phytosaurs**

228 A comparison with other phytosaurs shows that, while similar to each other, the endocranial

229 anatomy of *Ebrachosuchus neukami* and *Parasuchus angustifrons* differs in several aspects from

230 that of more derived taxa (Fig. 7). However, it should be noted that accurate comparisons are

231 exacerbated by the scarcity of detailed reconstructions of endocasts. Existing reconstructions are

232 mostly based on physical casts (natural and artificial) or interpretive drawings (Cope, 1888;

233 Case, 1928; Mehl, 1928; Camp, 1930; Chatterjee, 1978). All phytosaur endocasts appear to share

234 a basic bauplan with the individual brain regions arranged longitudinally (in contrast to a more

235 vertical arrangement such as seen in birds) and a mediolaterally narrow morphology. The

236 olfactory tracts are significantly elongate in all taxa (as far as preserved/reconstructed), making

237 up approximately half the length of the entire endocasts. Caudal to the olfactory tracts, the

238 various taxa show large differences in the orientation of the individual brain portions. Cephalic

239 and pontine flexure is very variable. While *Ebrachosuchus neukami* and *Parasuchus*

240 *angustifrons* share very large flexure angles (following Lautenschlager and Hübner, 2013) with

241 derived taxa, such as *Machaeroprosopus pristinus* and *Machaeroprosopus buceros*, the fore- and

242 mid-brain and the mid- and hind-brain appear to be almost perpendicular to each other in

243   *Smilosuchus gregori* and *Parasuchus hislopi*. However, although the studied specimens of

244   *Parasuchus angustifrons* (BSPG 1931 X 502) and *Ebrachosuchus neukami* (BSPG 1931 X 501)

245   are well preserved and mostly complete, they show signs of moderate dorsoventral compaction.

246   Retrodeformed endocast reconstructions exhibit cephalic and pontine flexures more similar to

247   *Machaeroprosopus mccauleyi* and *Parasuchus hislopi*. A significant difference is found in the

248   presence of a pineal organ or epiphysis dorsal to the cerebrum. A pineal organ has been

249   suggested to be present (Jaekel, 1910; Langston, 1949) and been reconstructed for the majority

250   of phytosaurs, but is absent in *Ebrachosuchus neukami* and *Parasuchus angustifrons*. The dorsal

251   expansion in the respective region in these taxa is interpreted in this study to represent parts of

252   the dural venous sinus or alternatively the paratympanic sinus, due to the rostral and lateral

253   expansion of this structure into parts of the braincase. Hopson (1979) similarly considered a

254   pineal organ in phytosaurs unlikely and suggested that the respective region in the endocranial

255   cavity housed a cartilaginous portion of the supraoccipital. Although reconstructed by Mehl

256   (1928), an enlarged epiphysis was reported to be absent in *Machaeroprosopus pristinus* in an as-

257   yet-unpublished recent study (Smith et al., 2010). Existing endocast reconstructions provide

258   ambiguous results regarding the presence of the epiphysis, but suggest that it may have

259   elaborated through phytosaur evolution (Fig. 7). However, considering its absence in modern

260   crocodilians, the epiphysis must have been lost at some stage prior to the origin of the

261   crocodilian crown group.

262   Similar to the actual brain endocast, the endosseous labyrinths show, as far as

263   reconstructed, subtle differences between different phytosaurian taxa. The vestibular part of the

264   labyrinth of *Ebrachosuchus neukami* and *Parasuchus angustifrons* is rostrocaudally longer than

265   dorsoventrally high, whereas it seems to have more uniform dimensions in *Machaeroprosopus*

266 *mccauleyi* and *Leptosuchus* sp. Again, this is to some extent a result of dorsoventral

267 compression. The retrodeformed endosseous labyrinths of *Ebrachosuchus neukami* and

268 *Parasuchus angustifrons* are more similar to the labyrinth of *Leptosuchus* sp. It should be noted,

269 though, that the retrodeformation is based on dorsoventral scaling of the complete skull and

270 endocast, respectively. However, the opisthotic and the paroccipital, which house the endosseous

271 labyrinth, might not have suffered the same amount of compression as the complete skull.

272 Furthermore, the scarcity of reconstructed and preserved natural labyrinthine endocasts

273 confounds wider comparisons.

274

275 **Comparison with Crocodyliformes**

276   As in comparison with other phytosaurs, the endocranial anatomy of *Ebrachosuchus*

277 *neukami* and *Parasuchus angustifrons* shares a basic bauplan with most Crocodyliformes in the

278 form of a longitudinally arranged and elongate brain architecture thought to be plesiomorphic for

279 the whole lineage (Hopson, 1979). As in phytosaurs, the olfactory tracts are elongate in extant

280 crocodylians, including *Alligator mississippiensis* (Witmer and Ridgely, 2008)*, Crocodylus*

281 *johnstoni* (Witmer et al., 2008) and *Crocodylus moreleti* (Franzosa, 2004), as well as in several

282 phylogenetically distinct Mesozoic longirostrine crocodylomorphs, such as the neosuchian

283 *Pholidosaurus* (Edinger, 1938; Hopson, 1979) and the metriorhynchid *Cricosaurus araucanensis*

284 (Herrera et al., 2013). In contrast to phytosaurs, the cerebral hemispheres are prominent and

285 mediolaterally enlarged in most Crocodyliformes (Wharton, 2000; Franzosa, 2004; George and

286 Holliday, 2013). Extant crocodylians possess an enlarged dural venous sinus covering the

287 endocast dorsally (Witmer et al., 2008), which has been interpreted to be present in fossil

288 Mesoeucrocodylia (Hopson, 1979; Wharton, 2000). Where preserved or reconstructed, the

289   endosseous labyrinths show a dorsoventrally compressed vestibular region and short cochlear

290   ducts in Crocodyliformes (Franzosa, 2004; Witmer et al., 2008), similar to *Ebrachosuchus*

291   *neukami* and *Parasuchus angustifrons*.

292   Paranasal sinuses have been reconstructed only for a handful of extant and extinct

293   Crocodyliformes (e.g. *Alligator mississippiensis*, *Cricosaurus araucanensis*), which limits

294   comparisons of these structures. A clear difference is found in the size of the antorbital sinus. In

295   *Ebrachosuchus neukami* and *Parasuchus angustifrons* the antorbital sinus is enlarged, but it is

296   considerably smaller in Crocodyliformes (Witmer and Ridgely, 2008; Herrera et al., 2013). Due

297   to the position of the external nares the airway is short in the studied phytosaurs. In the

298   longirostrine metriorhynchid *Cricosaurus araucanensis*, the rostrum comprises the airway for its

299   entire length (Herrera et al., 2013), whereas the comparable region was likely filled by a

300   premaxillary sinus in phytosaurs.

301

302   **DISCUSSION**

303   The reconstruction of the endocranial anatomy of *Ebrachosuchus neukami* and

304   *Parasuchus angustifrons* suggests that the general bauplan of pseudosuchian brain architecture

305   was already established in Phytosauria. Plesiomorphic characters, such as elongate olfactory

306   tracts, a mediolaterally narrow and serially aligned brain and a comparably small cerebral region,

307   are largely retained in other phytosaurs, but also in most Crocodyliformes. In contrast, features

308   that occur in the evolution of avemetatarsalian archosaurs such as a rearrangement of the brain

309   architecture, a hyperinflated cerebrum and a reduction of the olfactory apparatus (Zelenitsky et

310   al., 2011; Balanoff et al., 2013) are absent in the pseudosuchian lineage.

311   However, in spite of these overall similarities there are a number of differences present in

312   the endocranial anatomy when comparisons are made between various phytosaurian taxa, but

313   also in comparison to the (admittedly small number of) available endocranial reconstructions of

314   Crocodyliformes. Whether these reflect subtle ecological or behavioural adaptations,

315   intraspecific variation or interpretive artefacts is difficult to discern. The small sample size and

316   lack of detailed, three-dimensional reconstructions currently prevents rigorous tests of the latter

317   two possibilities. It is generally assumed that the osteological similarities between phytosaurs

318   and longirostrine Crocodyliformes are the result of convergent evolution and the adaptation to

319   the same habitat and/or diet (e.g. Camp, 1930; Hunt, 1989). Similarities or differences in the

320   endocranial anatomy could therefore indicate adaptive changes of key structures. Apart from the

321   plesiomorphic morphology of the brain inherent to both phytosaurs and Crocodyliformes, both

322   groups share a dorsoventrally flattened and rostrocaudally expanded morphology of the

323   vestibular apparatus of the inner ear. Such an increase in the aspect ratio of the vertical

324   semicircular canals has been associated with an adaptation to an aquatic environment (Georgi

325   and Sipla, 2008) and is found also in other marine reptiles (Neenan and Scheyer, 2012). It

326   therefore possible that the endocranial anatomy in phytosaurs and longirostrine Crocodyliformes

327   follows a shared plesiomorphic pattern that has been convergently modified in response to

328   similar sensory adaptations. Additional sampling of phytosaur and fossil crocodyliform

329   endocasts and more refined palaeobehavioural and palaeoecological data will be required to

330   provide a more definitive assessment of this hypothesis.

331

332   **CONCLUSIONS**

333   The digital reconstruction of the brain, inner ear, neurovascular and sinus morphology of

334   the two non-mystriosuchine phytosaurs *Parasuchus angustifrons* and *Ebrachosuchus neukami*

335   offers new insights into the endocranial anatomy and evolution of Phytosauria. The endocasts of

336   both taxa are very similar to each other in their rostrocaudally elongate morphology, with long

337   olfactory tracts, weakly demarcated cerebral regions and dorsoventrally short endosseous

338   labyrinths. Several sinuses, including large antorbital sinuses and prominent dural venous

339   sinuses, were reconstructed. Comparisons with published endocranial reconstructions of other,

340   more derived, phytosaurian taxa demonstrate a substantial morphological variability, most

341   pronounced in the cephalic and pontine flexure and the presence of a pineal organ. Endocranial

342   characters that are found across all phytosaurs, as far as preserved, include the elongate olfactory

343   tract and a serially arranged brain architecture. As far as allowed by the limited available

344   comparative data, these features appear to be shared with members of the clade Crocodyliformes.

345   However, the scarcity of reconstructed endocasts for phytosaurs and crocodyliforms, as well as

346   preservational artefacts, confound large-scale comparisons and provide an impetus for further

347   future work on the endocranial anatomy and evolution of these clades.

348

349   **ACKNOWLEDGEMENTS**

353

354   **LITERATURE CITED**

355   Anderson HT. 1936. The jaw musculature of the phytosaur *Machaeroprosopus*. *Journal of*

356   *Morphology* 59:549-587.

357   Balanoff AM, Bever GS, Rowe TB, and Norell MA. 2013. Evolutionary origins of the avian

358   brain. *Nature* 501:93-96.

359   Brochu CA. 2001. Crocodylian snouts in space and time: phylogenetic approaches toward

360   adaptive radiation. . *American Zoologist* 41:564-585.

361   Brusatte SL, Benton MJ, Desojo JB, and Langer MC. 2010. The higher−level phylogeny of

362   Archosauria (Tetrapoda: Diapsida). *Journal of Systematic Palaeontology* 8:3-47.

363   Buffetaut E. 1993. Phytosaurs in time and space. In: Mazin JM, and Pinna G, eds. *Evolution,*

364   *Ecology and Biogeography of the Triassic Reptiles*. Milan: Paleontologia Lombarda della

365   Societa Italiana di Scienze Naturali e del Museo Civico di Storia Naturale, 39-44.

366   Butler RJ, Rauhut OWM, Stocker MR, and Bronowicz R. 2014. Redescription of the phytosaurs

367   *Paleorhinus* ('*Francosuchus*') *angustifrons* and *Ebrachosuchus neukami* from Germany,

368   with implications for Late Triassic biochronology. *Zoological Journal of the Linnean*

369   *Society* 170:155-208.

370   Camp CL. 1930. A study of the phytosaurs with description of new material from western North

371   America. *Memoirs of the University of California* 10:1-174.

372   Case EC. 1928. An endocranial cast of a phytosaur from the Upper Triassic beds of western

373   Texas. *Journal of Comparative Neurology* 45:161-168.

374   Chatterjee S. 1978. A primitive parasuchid (Phytosaur) reptile from the Upper Triassic Maleri

375   Formation of India. *Palaeontology* 21:83-127.

376   Cope ED. 1888. The pineal eye in extinct vertebrates. *The American Naturalist* 22:914-917.

377   Edinger T. 1938. Über Steinkerne von Hirn- und Ohr-Höhlen der Mesosuchier *Goniopholis* und

378   *Pholidosaurus* aus dem Bückeburger Wealden. *Acta Zoologica* 19:467-505.

379   Ezcurra MD. 2016. The phylogenetic relationships of basal archosauromorphs, with an emphasis

380   on the systematics of proterosuchian archosauriforms. *PeerJ* 4:e1778. 10.7717/peerj.1778

381   Franzosa JW. 2004. Evolution of the brain in Theropoda (Dinosauria) Unpublished PhD thesis.

382   University of Texas.

383   George ID, and Holliday CM. 2013. Trigeminal nerve morphology in *Alligator mississippiensis*

384   and its significance for crocodyliform facial sensation and evolution. *Anat Rec* 296:670-

385   680.

386   Georgi JA, and Sipla JS. 2008. Comparative and functional anatomy of balance in aquatic

387   reptiles and birds. In: Thewissen JGM, and Nummela S, eds. *Sensory Evolution on the*

388   *Threshold: Adaptations in Secondarily Aquatic Vertebrates*. Berkeley, California.:

389   University of California Press, 233-256.

390   Herrera Y, Fernandez MS, and Gasparini Z. 2013. The snout of *Cricosaurus araucanensis*: a

391   case study in novel anatomy of the nasal region of metriorhynchids. *Lethaia* 46:331-340.

392   Holloway WL, Claeson KM, and O'Keefe FR. 2013. A virtual phytosaur endocast and its

393   implications for sensory system evolution in archosaurs. *Journal of Vertebrate*

394   *Paleontology* 33:848-857.

395   Hopson JA. 1979. Paleoneurology. In: Gans C, Northcutt RC, and Ulinski P, eds. *Biology of the*

396   *Reptilia*. New York: Academic Press, 39-146.

397   Hungerbühler A. 2002. The Late Triassic phytosaur *Mystriosuchus westphali*, with a revision of

398   the genus. *Palaeontology* 45:377-418.

399   Hunt AP. 1989. Cranial morphology and ecology among phytosaurs. In: Lucas SG, and Hunt

400   AP, eds. *Dawn of the Age of Dinosaurs in the American Southwest*. Albuquerque: New

401   Mexico Museum of Natural History, 349-354.

402 Jaekel O. 1910. Ueber einen neuen Belodonten aus dem Buntsandstein von Bernberg.

403   *Sitzungsberichte Gesellschaft naturforschender Freunde zu Berlin* 5:197-229.

404 Kammerer CF, Butler RJ, Bandyopadhyay S, and Stocker MR. 2016. Relationships of the Indian

405   phytosaur *Parasuchus hislopi* Lydekker, 1885. *Papers in Palaeontology* 2:1–23.

406 Kuhn O. 1936. Weitere Parasuchier und Labyrinthodonten aus dem Blasensandstein des

407   mittleren Keuper von Ebrach. Palaeontographica Abteilung A 83: 61–98.

408 Langston WL, Jr. 1949. A new species of *Paleorhinus* from the Triassic of Texas. *American*

409   *Journal of Science* 247:324-341.

410 Lautenschlager S. 2014. Palaeontology in the third dimension: a comprehensive guide for the

411   integration of three-dimensional content in publications. *Paläontologische Zeitschrift*

412   88:111-121.

413 Lautenschlager S, and Hübner T. 2013. Ontogenetic trajectories in the ornithischian

414   endocranium. *Journal of Evolutionary Biology* 26:2044-2050.

415 Leitch DB, and Catania KC. 2012. Structure, innervation and response properties of

416   integumentary sensory organs in crocodilians. *Journal of Experimental Biology*

417   215:4217-4230.

418 Mehl MG. 1928. *Pseudopalatus pristinus*, a new genus and species of phytosaurs from Arizona.

419   *University of Missouri Studies* 3:1-22.

420 Neenan JM, and Scheyer TM. 2012. The braincase and inner ear of *Placodus gigas*

421   (Sauropterygia, Placodontia)—a new reconstruction based on micro-computed

422   tomographic data. *Journal of Vertebrate Paleontology* 32:1350-1357.

423 Nesbitt SJ. 2011. The early evolution of archosaurs: relationships and the origin of major clades.

424   *Bulletin of the American Museum of Natural History* 352:1-292.

425   Parrish JM. 1986. Structure and function of the tarsus in the phytosaurs (Reptilia: Archosauria).

426   In: Padian K, ed. *The beginning of the Age of Dinosaurs: Faunal Change Across the*

427   *Triassic-Jurassic Boundary*. Cambridge: Cambridge University Press, 35-43.

428   Parrish JM. 1993. Phylogeny of the Crocodylotarsi, with reference to archosaurian and

429   crurotarsan monophyly. *Journal of Vertebrate Paleontology* 13:287-308.

430   Pierce SE, Angielczyk KD, and Rayfield EJ. 2008. Patterns of morphospace occupation and

431   mechanical performance in extant crocodilian skulls: a combined geometric

432   morphometric and finite element modeling approach. *Journal of Morphology* 269:840-

433   864.

434   Renesto S, and Lombardo C. 1999. Structure of the tail of a phytosaur (Reptilia, Archosauria)

435   from the Norian (Late Triassic) of Lombardy (northern Italy). *Rivista Italiana di*

436   *Paleontologia e Stratigrafia* 105:135-144.

437   Sereno PC. 1991. Basal archosaurs: phylogenetic relationships and functional implications.

438   *Society of Vertebrate Paleontology Memoir* 2:1-53.

439   Smith D, Sanders R, Parker W, and Cavanaugh J. 2010. The endocranium, inner ear, and

440   pneumatic structure of the Upper Triassic phytosaur *Pseudopalatus pristinus*. *Journal of*

441   *Vertebrate Paleontology, SVP Program and Abstracts Book*:176A.

442   Stocker MR, and Butler RJ. 2013. Phytosauria. *Geological Society, London, Special Publications*

443   379:91-117.

444   Westphal F. 1976. Phytosauria. In: O K, ed. *Handbuch der Paläoherpetologie*. Stuttgart: Gustav

445   Fischer Verlag, 99-120.

446   Wharton DS. 2000. An enlarged endocranial venous system in *Steneosaurus pictaviensis*

447   (Crocodylia: Thalattosuchia) from the Upper Jurassic of Les Lourdines, France. *Comptes*

448   *Rendus de l'Académie des Sciences - Series IIA - Earth and Planetary Science* 331:221-

449   226.

450   Witmer LM. 1997. Craniofacial air sinus systems. In: Currie PJ, and Padian K, eds. *The*

451   *Encyclopedia of Dinosaurs*. New York: Academic Press, 151-159.

452   Witmer LM, Chatterjee S, Franzosa JW, and Rowe T. 2003. Neuroanatomy of flying reptiles and

453   implications for flight, posture and behaviour. *Nature* 425:950-953.

454   Witmer LM, and Ridgely RC. 2008. The paranasal air sinuses of predatory and armored

455   dinosaurs (Archosauria: Theropoda and Ankylosauria) and their contribution to cephalic

456   structure. *The Anatomical Record* 291:1362-1388.

457   Witmer LM, and Ridgely RC. 2009. New insights into the brain, braincase, and ear region of

458   tyrannosaurs (Dinosauria, Theropoda), with implications for sensory organization and

459   behavior. *The Anatomical Record* 292:1266-1296.

460   Witmer LM, Ridgely RC, Dufeau DL, and Semones MC. 2008. Using CT to peer into the past:

461   3D visualization of the brain and ear regions of birds, crocodiles, and nonavian dinosaurs.

462   In: Endo H, and Frey R, eds. *Anatomical Imaging - Towards a new morphology*. Tokyo,

463   Berlin, Heidelberg, New York: Springer, 67-87.

464   Witzmann F, Schwarz-Wings D, Hampe O, Fritsch G, and Asbach P. 2014. Evidence of

465   spondyloarthropathy in the spine of a phytosaur (Reptilia: Archosauriformes) from the

466   Late Triassic of Halberstadt, Germany. *PLoS ONE* 9:e85511.

467   Zelenitsky DK, Therrien F, Ridgely RC, McGee AR, and Witmer LM. 2011. Evolution of

468   olfaction in non-avian theropod dinosaurs and birds. *Proceedings of the Royal Society*

469   *London, Series B* 278:3625-3634.

471 **FIGURE CAPTIONS**

472 **Figure 1 Studied phytosaurian taxa.** Physical specimen (left) and digital representation (right)

473 of (**A**) *Parasuchus angustifrons* (BSPG 1931 X 502) and (**B**) *Ebrachosuchus neukami* (BSPG

474 1931 X 501).

475

476 **Figure 2 Endocranial anatomy of *Parasuchus angustifrons* (BSPG 1931 X 502).** Endocast of

477 brain and endosseous labyrinth in (**A**) left lateral and (**B**) dorsal view. Endocast in situ in (**C**) left

478 lateral and (**D**) dorsal view with bone rendered semi-transparent.

479

480 **Figure 3. Endocranial anatomy of *Ebrachosuchus neukami* (BSPG 1931 X 501).** Endocast of

481 brain and endosseous labyrinth in (**A**) left lateral and (**B**) dorsal view. Endocast in situ in (**C**) left

482 lateral and (**D**) dorsal view with bone rendered semi-transparent.

483

484 **Figure 4 Paranasal sinuses of *Parasuchus angustifrons* (BSPG 1931 X 502)**. Sinuses in (**A**)

485 and (**B**) in rostrolateral view and (**C**) and (**D**) dorsal view. Sinuses in (**B**) and (**D**) in situ with

486 bone rendered semi-transparent.

487

488 **Figure 5 Paranasal sinuses of *Ebrachosuchus neukami* (BSPG 1931 X 501).** Sinuses in (**A**)

489 and (**B**) in rostrolateral view and (**C**) and (**D**) dorsal view. Sinuses in (**B**) and (**D**) in situ with

490 bone rendered semi-transparent.

491

492   **Figure 6 Endosseous labyrinths.** *Parasuchus angustifrons* (BSPG 1931 X 502) (A) left

493   labyrinth, (B) right labyrinth. *Ebrachosuchus neukami* (BSPG 1931 X 501) (C) left labyrinth, (D)

494   right labyrinth. Each from left to right in lateral, caudal, rostral, medial and dorsal view. Parts

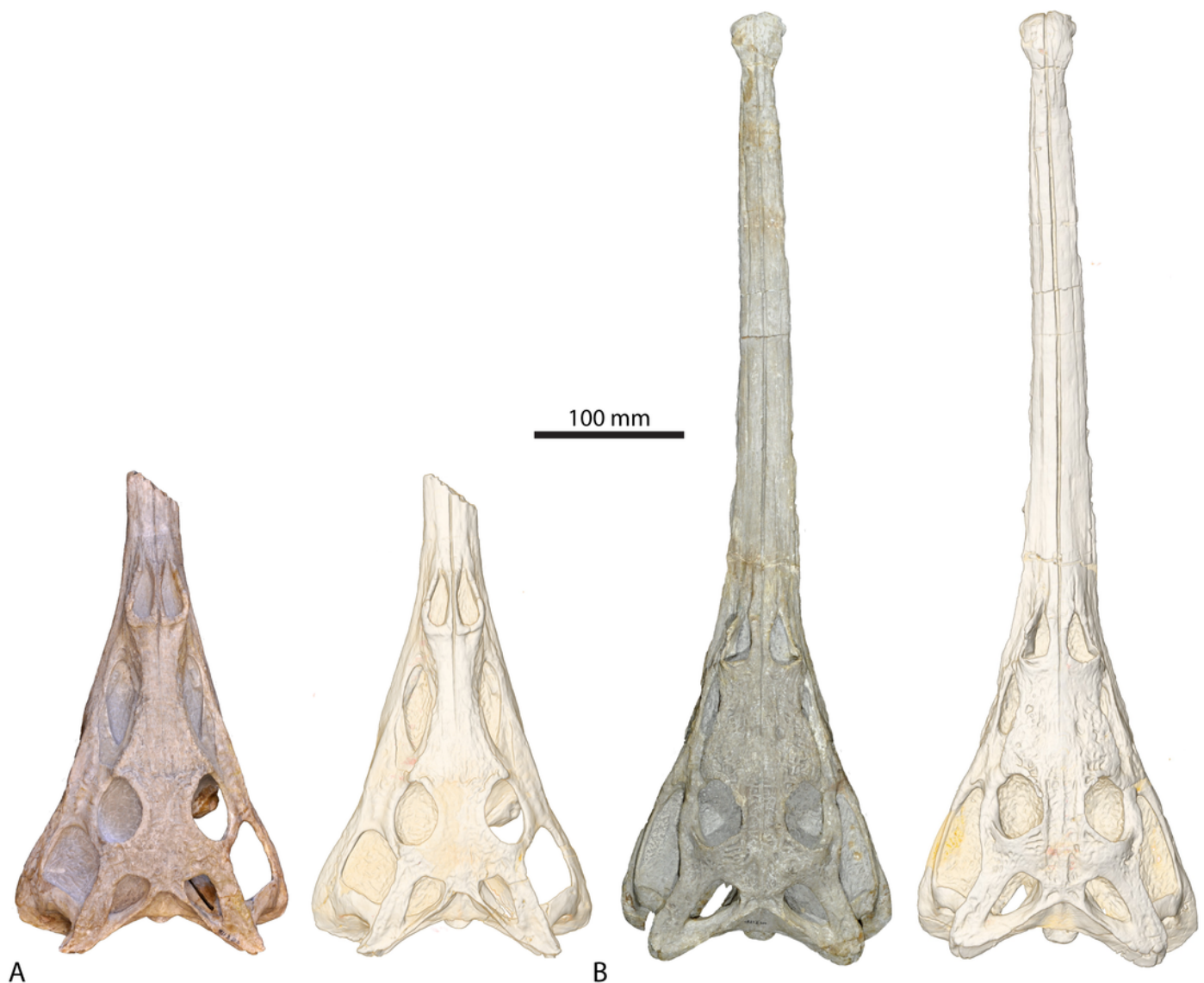495   reconstructed and reflected from the opposite side (where preserved) shown in different colour.

496

497   **Figure 7 Endocranial anatomy of different phytosaurian taxa.** Comparisons based on

498   existing endocasts and endocast reconstruction redrawn from Cope (1888), Case (1928), Mehl

499   (1928), Camp (1930), Chatterjee (1978) and Holloway et al. (2013). Time-calibrated phylogeny

500   based on Stocker and Butler (2013), Kammerer et al. (2016) and Ezcurra (2016). Endocasts of

501   *Parasuchus angustifrons* and *Ebrachosuchus neukami* shown after retrodeformation.

502

503   **Figure 8 Retrodeformation of studied taxa.** (A) Complete and undistorted skull of *Parasuchus*

504   *hislopi* (ISI R42) used as a guide for retrodeformation of (B) *Parasuchus angustifrons* (BSPG

505   1931 X 502) and (C) *Ebrachosuchus neukami* (BSPG 1931 X 501). Original (top) and

506   retrodeformed (bottom) skull and respective endocasts shown for each taxon.
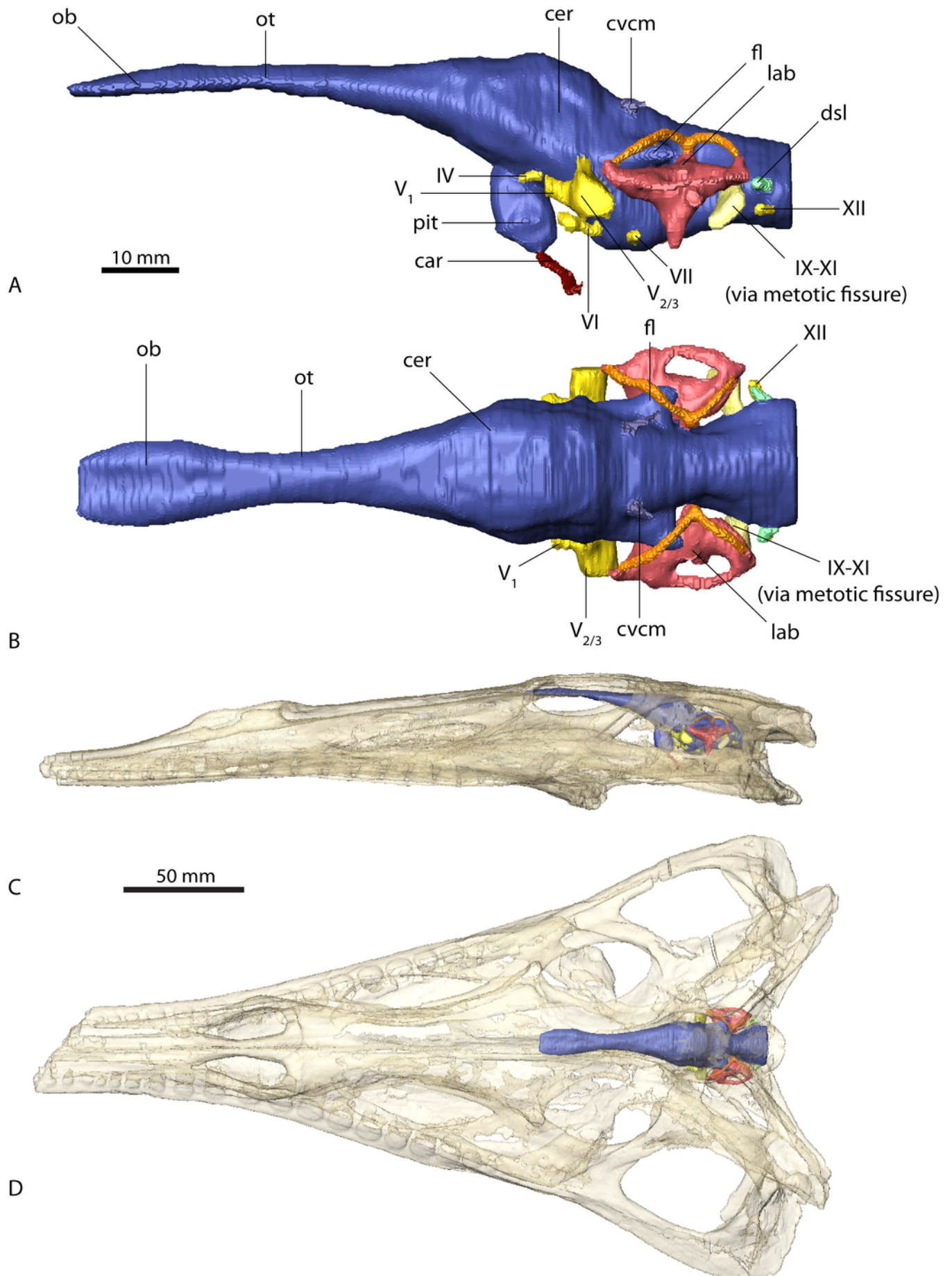
Figure 1

Studied phytosaurian taxa.

Physical specimen (left) and digital representation (right) of (A) *Parasuchus angustifrons* (BSPG 1931 X 502) and (B) *Ebrachosuchus neukami* (BSPG 1931 X 501).

Figure 2

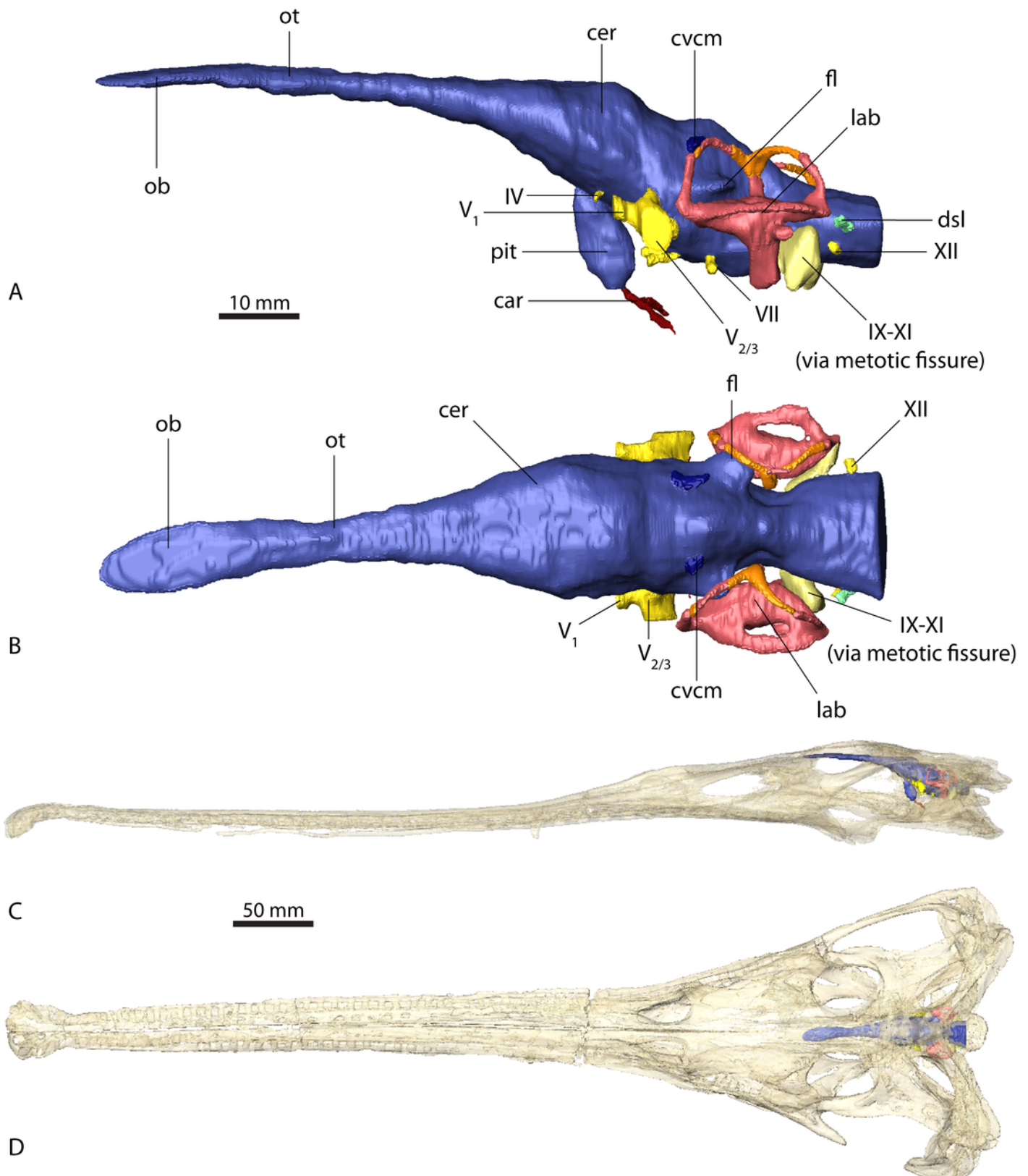Endocranial anatomy of *Parasuchus angustifrons* (BSPG 1931 X 502).
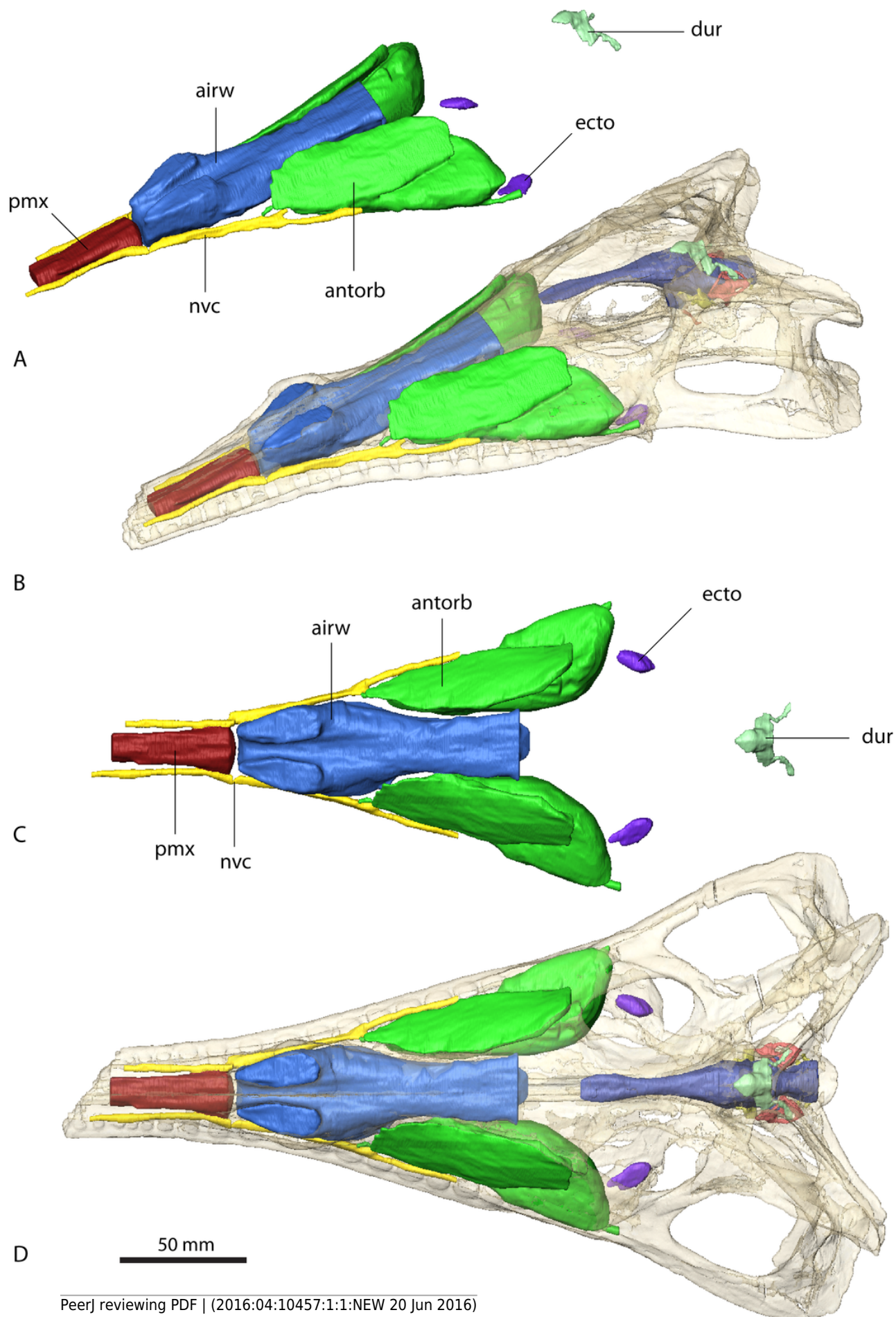
Endocast of brain and endosseous labyrinth in (A) left lateral and (B) dorsal view. Endocast in situ in (C) left lateral and (D) dorsal view with bone rendered semi-transparent.

Figure 3

Endocranial anatomy of *Ebrachosuchus neukami* (BSPG 1931 X 501).

Endocast of brain and endosseous labyrinth in (A) left lateral and (B) dorsal view. Endocast in situ in (C) left lateral and (D) dorsal view with bone rendered semi-transparent.

Figure 4

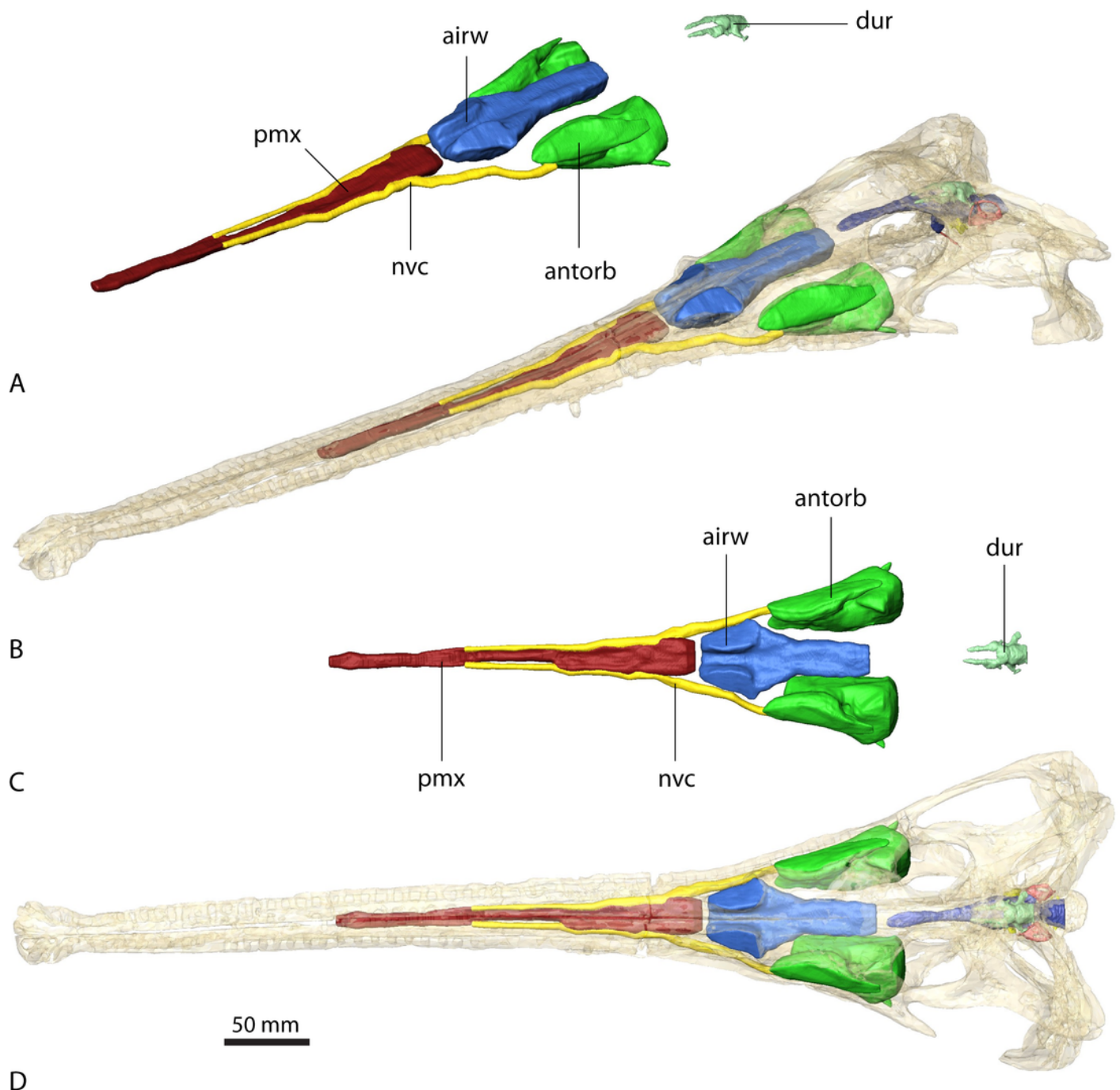Paranasal sinuses of *Parasuchus angustifrons* (BSPG 1931 X 502).

Sinuses in (A) and (B) in rostrolateral view and (C) and (D) dorsal view. Sinuses in (B) and (D) in situ with bone rendered semi-transparent.

Figure 5

Paranasal sinuses of *Ebrachosuchus neukami* (BSPG 1931 X 501).

Sinuses in (A) and (B) in rostrolateral view and (C) and (D) dorsal view. Sinuses in (B) and (D) in situ with bone rendered semi-transparent.
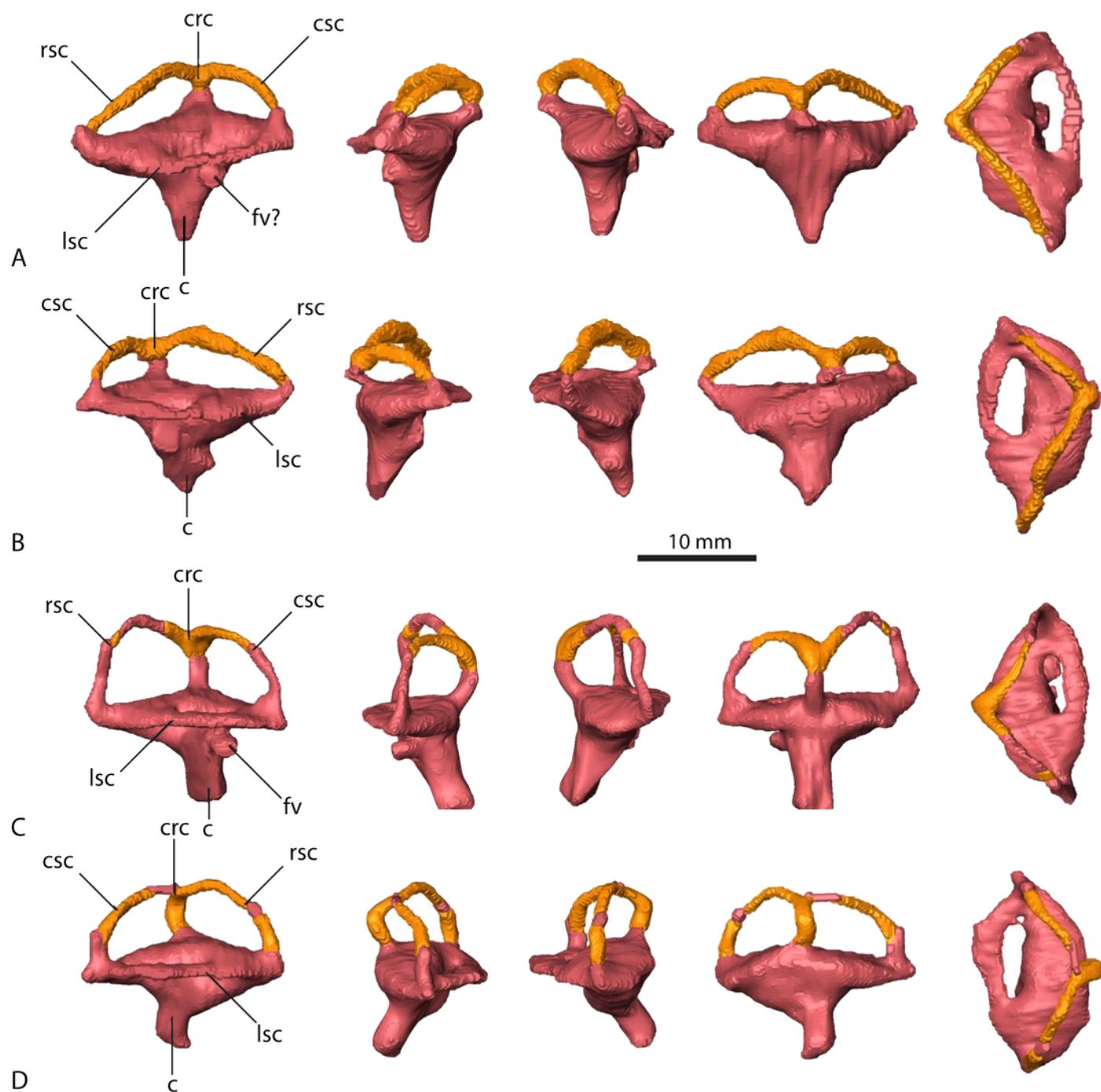
PeerJ

Figure 6

Endosseous labyrinths.

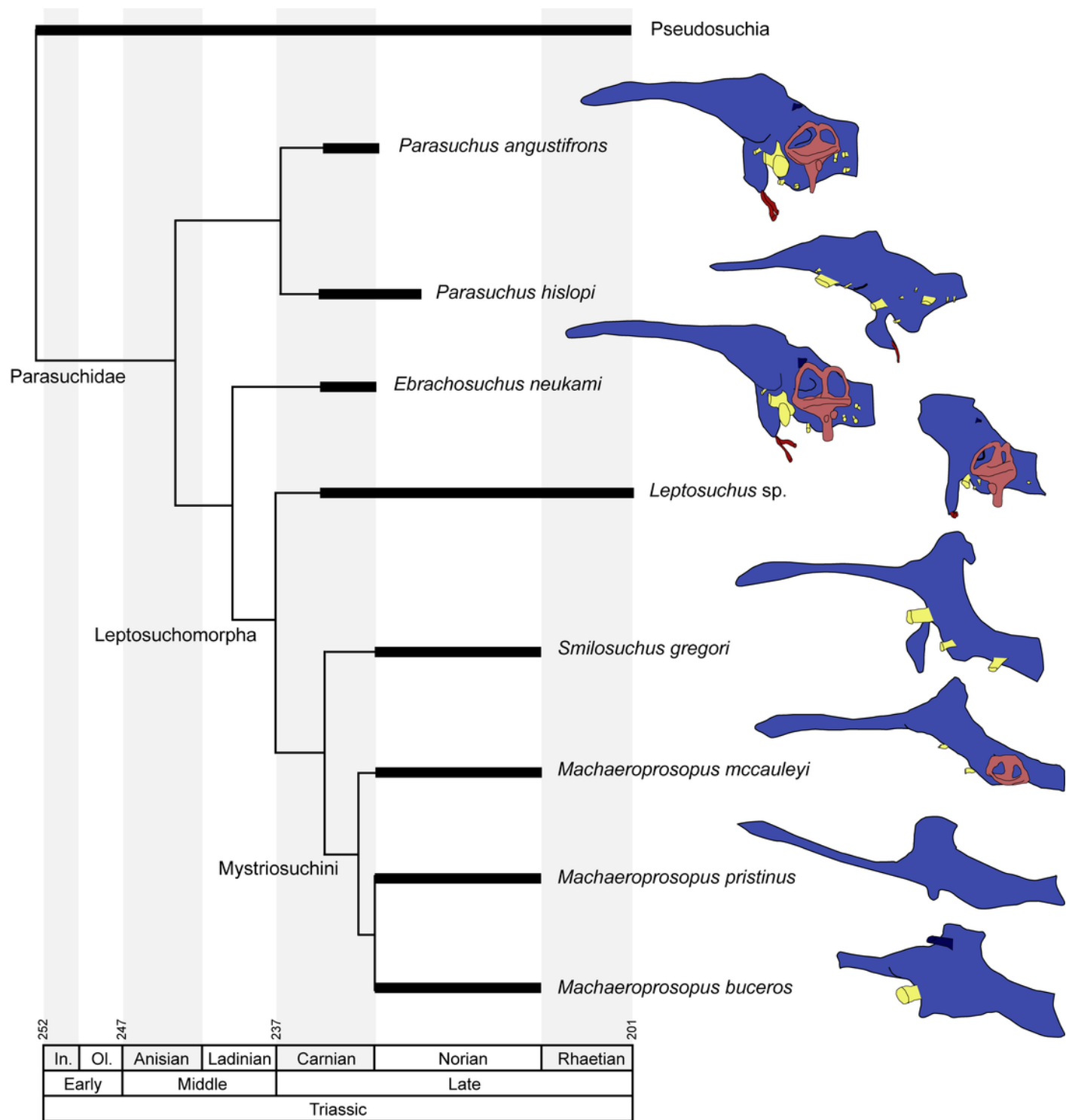*Parasuchus angustifrons* (BSPG 1931 X 502) (A) left labyrinth, (B) right labyrinth. *Ebrachosuchus neukami* (BSPG 1931 X 501) (C) left labyrinth, (D) right labyrinth. Each from left to right in lateral, caudal, rostral, medial and dorsal view. Parts reconstructed and reflected from the opposite side (where preserved) shown in different colour.

Figure 7

Endocranial anatomy of different phytosaurian taxa.

Comparisons based on existing endocasts and endocast reconstruction redrawn from Cope (1888), Case (1928), Mehl (1928), Camp (1930), Chatterjee (1978) and Holloway et al. (2013). Time-calibrated phylogeny based on Stocker and Butler (2013), Kammerer et al. (2016) and Ezcurra (2016). Endocasts of *Parasuchus angustifrons* and *Ebrachosuchus neukami* shown after retrodeformation.

Pseudosuchia

Parasuchus angustifrons

Parasuchus hislopi

Parasuchidae

Ebrachosuchus neukami

Leptosuchus sp.

Leptosuchomorpha

Smilosuchus gregori

Machaeroprosopus mccauleyi

Mystriosuchini

Machaeroprosopus pristinus

Machaeroprosopus buceros

In.	Ol.	Anisian	Ladinian	Carnian	Norian	Rhaetian
Early		Middle		Late		
Triassic						

252 247 237 201

Figure 8

Retrodeformation of studied taxa.

(A) Complete and undistorted skull of *Parasuchus hislopi* (ISI R42) used as a guide for
retrodeformation of (B) *Parasuchus angustifrons* (BSPG 1931 X 502) and (C) *Ebrachosuchus
neukami* (BSPG 1931 X 501). Original (top) and retrodeformed (bottom) skull and respective
endocasts shown for each taxon.